Molecular Imaging as In Vivo Molecular Pathology for Gastroenteropancreatic Neuroendocrine Tumors: Implications for Follow-Up After Therapy

Eric P. Krenning, MD, PhD[1,2]; Roelf Valkema, MD, PhD[1]; Dik J. Kwekkeboom, MD, PhD[1]; Wouter W. de Herder, MD, PhD[2]; Casper H.J. van Eijck[3], MD, PhD; Marion de Jong, PhD[1]; Stanislas Pauwels, MD, PhD[4]; and Jean-Claude Reubi, MD, PhD[5]

[1]Department of Nuclear Medicine, Erasmus Medical Center, Rotterdam, The Netherlands; [2]Department of Internal Medicine, Erasmus Medical Center, Rotterdam, The Netherlands; [3]Department of Surgery, Erasmus Medical Center, Rotterdam, The Netherlands; [4]Department of Nuclear Medicine, Université Catholique de Louvain, Brussels, Belgium; and [5]Division of Cell Biology and Experimental Cancer Research, Institute of Pathology, University of Bern, Switzerland

Peptide receptor scintigraphy in combination with anatomic imaging methods such as CT can be regarded as molecular imaging. It offers insight into the variability of somatostatin receptor expression in neuroendocrine tumor lesions within a patient. The somatostatin receptor status of all tumors in a patient is an important issue, because receptor-negative lesions may be poorly differentiated and characterized by aggressive growth and poor prognosis, with consequences for the choice of therapy. **Methods:** Follow-up studies of 3 patients with gastroenteropancreatic neuroendocrine tumors who had been previously treated with peptide receptor radionuclide therapy (PRRT) are presented. **Results:** Patient 1 had a mixed response after treatment with ^{90}Y-1,4,7,10-tetraazacyclododecane-*N,N′,N″,N‴*-tetraacetic acid^{0} (DOTA),Tyr^{3}-octreotide. The response included fibrosis and a low rate of mitosis in receptor-positive lesions that had decreased in volume after treatment and vital tumor cells and a high rate of mitosis in receptor-negative lesions that had grown since the start of treatment. Patient 2 had a good clinical and biochemical response after PRRT with [^{177}Lu-DOTA^{0},Tyr^{3}]octreotate (^{177}Lu-DOTATATE), with disappearance of ^{111}In-pentetreotide uptake on follow-up scans, whereas on CT the size of the lesions remained unchanged, possibly indicating tumor necrosis. Patient 3 had a complete remission after PRRT with ^{177}Lu-DOTATATE but subsequently relapsed with many receptor-negative metastases, requiring intensive chemotherapy. **Conclusion:** Although biopsy is required for initial diagnosis and treatment planning, noninvasive molecular imaging may evolve into in vivo molecular pathology in selected groups of patients, especially in treatment follow-up.

Received Sep. 15, 2004; revision accepted Sep. 17, 2004.

For correspondence or reprints contact: Eric P. Krenning, MD, PhD, Department of Nuclear Medicine, Erasmus Medical Center, Dr. Molewaterplein 40, 3015 GD Rotterdam, The Netherlands.

E-mail: E.P.Krenning@erasmusmc.nl

Key Words: neuroendocrine tumor; pathology; peptide; peptide receptor radiation therapy

J Nucl Med 2005; 46:76S–82S

Nuclear oncology using SPECT and PET is able to show the presence of peptide receptors on gastroenteropancreatic (GEP) neuroendocrine tumors (NETs) in vivo. Functional imaging techniques, such as peptide receptor scintigraphy (PRS), in conjunction with anatomic techniques like CT and MR imaging, enable mapping of the presence of peptide receptors in tumors within individual patients. This combination of functional and anatomic imaging is also referred to as molecular imaging. More peptides are emerging for this goal, and these will be applied for imaging of the receptor status in various types of tumors (*1*). Radiolabeled peptides are also being successfully applied to peptide receptor radionuclide therapy (PRRT) of GEP NETs.

Tumor heterogeneity must be considered a major issue for PRS and PRRT, because it is likely that only peptide receptor–positive lesions will be imaged by PRS or respond to PRRT. Moreover, it is well known that the prognosis is worse in patients with GEP NETs that have characteristics of dedifferentiation (*2*). Therefore, knowledge of the existence of such dedifferentiated tumors or areas within a differentiated tumor may be crucial for the choice of therapy. In vitro autoradiography studies using radiolabeled somatostatin analogs have shown that, in general, the primary lesion as well as metastases of well-differentiated GEP NETs express somatostatin receptors. Little information is available about the coexistence of dedifferentiated GEP NET cells within individual differentiated tumors. However, receptor autoradiography is able to detect re-

stricted areas of heterogeneous receptor distribution that can be assumed to represent areas of distinct differentiation and biologic behavior. In vitro receptor techniques are usually hampered by the fact they provide information only about a restricted part of a patient's neoplasm rather than the whole tumor and all metastases. Knowledge of potential receptor heterogeneity between metastases in a single patient is often not available, simply because it is impossible to obtain tissue samples from all lesions. The advantage of nuclear medicine is that it can visualize the whole lesion by virtue of studying a variety of molecular processes with high sensitivity, very often with similar molecules as being used in pathology. In a certain sense, it can thus be applied as in vivo nuclear or molecular pathology. Mapping of these results with those of anatomic imaging may give individualized information about heterogeneity between metastases.

On the other hand, all imaging techniques fail to localize very small lesions. Therefore these techniques and pathology are unable to provide molecular information about occult disease and will miss small heterogeneous foci.

After studying the degree of differentiation of GEP NETs on the basis of histologic criteria, it became clear that antitumor responses to chemotherapy were quite different in differentiated and dedifferentiated GEP NETs (*2,3*). Only the dedifferentiated tumors showed regression after a regimen of cisplatin and VP-16, and, unfortunately, this effect generally lasted less than 1 y. Analysis of such tumors by autoradiography using radiolabeled somatostatin analogs revealed that only differentiated tumors were somatostatin receptor–positive (*3,4*). Translating these findings to in vivo studies for PRS and PRRT using somatostatin analogs, it is likely most of the metastasized, differentiated GEP NETs are visible and treatable, provided the degree of uptake is sufficiently high. Indeed, a very high sensitivity for PRS in GEP NETs has been found by various groups (*7,8,11–14*).

Here we present several cases that illustrate how important and difficult the interpretation of molecular imaging can be for GEP NET during or after therapy. The strength of molecular imaging in the context of in vivo molecular pathology will be discussed.

PATIENTS

Patient 1

Patient 1 was a 59-y-old man seen in 1997 with diarrhea, flushes, and progressive upper abdominal pain caused by liver metastases of a carcinoid with increased urinary 5-hydroxyindoleacetic acid excretion. The ^{111}In-DTPA-octreotide scan (octreotide scan) showed high uptake in the liver lesions as well as in an intestinal lesion. CT was judged to be consistent with the octreotide scan with regard to somatostatin receptor positivity of the lesions (Table 1). From April to September 1998, the patient was treated with

TABLE 1
Summary of Results in 3 Patients with GEP NETs

Patient	Tumor	Assessment point	PRS	CT/MRI	Molecular imaging	Histology
1	1	Initial imaging	Missed	Missed	Missed	NA
		PRRT response	No SS receptors	PD	Dd: PD of NET or second tumor	
		PRRT follow-up				NET: sst2(−)
	2	Initial imaging	(+)	(+)	(+)	GEP NET
		PRRT response	Decrease in uptake	SD	SD (with necrosis/fibrosis?)	
		PRRT follow-up				Fibrosis,* occult NET; sst2 (+)
2		Initial imaging	(+)	(+)	(+)	GEP NET
		PRRT response	(+) → (−) = CR	SD	Dd: SD (necrosis/fibrosis?) or dedifferentiation	
		PRRT follow-up				Necrosis,* occult NET cells
3	Initial tumor	Initial imaging	(+)	(+)	(+)	GEP NET
		PRRT response	(+) → (−) = CR	CR	CR	
		PRRT follow-up				NA (conclusion was CR because of CI)
	Recurrence	Initial imaging	(−)	(+)	(+)	
		Chemo response	NA	PR	Dd: PR of NET or second tumor	
		PRRT follow-up				NET dedifferentiation

*More antitumor effect than indicated by CT/MRI.

SS = somatostatin; PD = progressive disease; Dd = differential diagnosis; + = positive; SD = stable disease; − = negative; CR = complete response; CI = conventional imaging; NA = not available.

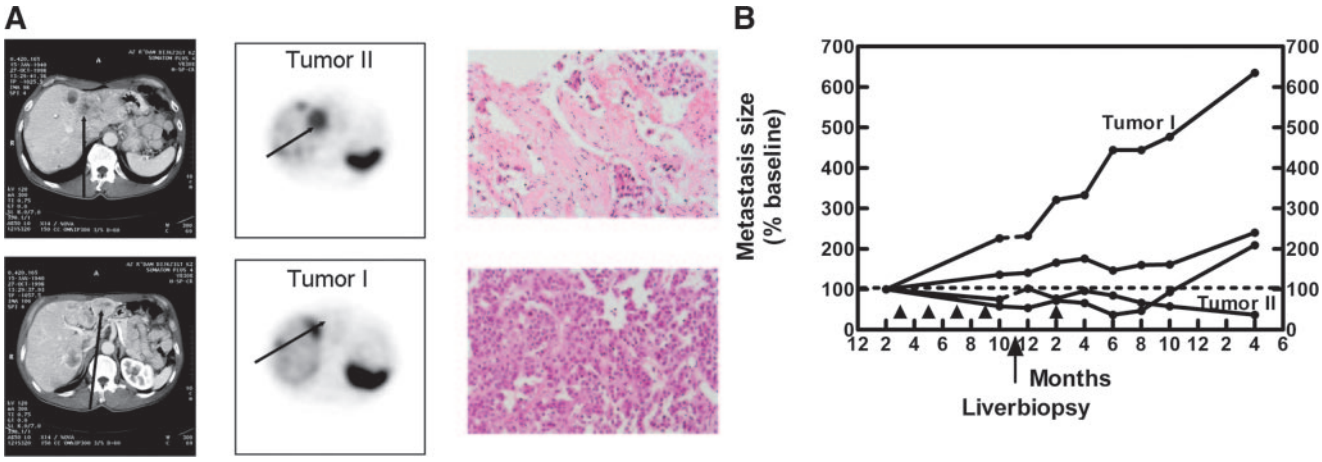

FIGURE 1. (A) Upper and lower panels represent transverse CT, SPECT, and hematoxylin and eosin histology of somatostatin receptor (SSR)-positive tumor 2 and SSR-negative tumor 1, respectively, in patient 1, after 4 cycles of PRRT. (B) Sizes of 4 hepatic lesions after PRRT with somatostatin analog (▲). Tumors above stippled line were not seen on octreotide scan, nor were the 2 tumors below this line; one of each was biopsied and depicted in (A).

6.7 GBq ^{90}Y-1,4,7,10-tetraazacyclododecane-*N,N′,N″,N‴*-tetraacetic acid^{0} (DOTA),Tyr^{3}-octreotide (^{90}Y-DOTATOC) in 4 treatment sessions and an additional treatment with 1.7 GBq in March 1999 (Fig. 1). Six weeks after the fourth cycle, the follow-up CT showed a mixed pattern of change in size in 4 indicator liver lesions: slight decreases in size in 2 tumors (which at baseline measured 14.4 and 27.0 cm^2) as well as clear increases in 2 other lesions (at baseline, 7.8 and 8.4 cm^2) (Fig. 1). At that point, however, it was recognized that the octreotide scan did not entirely correlate with CT imaging. Progressive lesions seemed to be cold and stable lesions hot on the octreotide scan. Dosimetry with ^{86}Y-DOTATOC PET revealed tumor doses for these positive lesions of at least 50 Gy (tumor volume based on PET, thus overestimating the tumor mass) (*5*). Only in retrospect and with the knowledge of follow-up CT imaging were cold lesions identified as small isodense lesions on the baseline CT. In December 1998, after 4 cycles of PRRT 2, needle biopsies were taken from each of 2 distinct tumor areas (hot and cold), which were evaluated for somatostatin receptor expression and morphologic and biochemical characteristics by a pathologist without knowledge of the in vivo scanning data (Table 2).

Tumor 1 in this patient was recognized as a compact group of neoplastic cells with moderate nuclear polymorphism, proliferating elements (3%–4% of monoclonal antibody MIB1-positive cells [Fig. 2]), with neuroendocrine differentiation (synaptophysin and CD56 strongly positive; chromogranin only weakly positive) and without noticeable intratumoral fibrosis. P-53 staining was negative. Few mitotic figures were seen. The somatostatin receptors measured with the ^{125}I-Tyr^{3}-octreotide ligand were mostly absent or expressed in very low amounts in certain tumor areas

TABLE 2
Morphological and Biochemical Characteristics of the 2 Tumor Samples from Patient 1

Characteristic	Tumor 1	Tumor 2
Density of SSR		
^{125}I-Tyr^{3}-octreotide binding (dpm/mg tissue) (range)	−/+ (0–648)	+++ (2,826–4,818)
Proliferation marker		
% of proliferating cells (MIB1)	3.4%	0.88%
Neuroendocrine/differentiation markers		
Synaptophysin	+++	+++
CD56	++	++
Chromogranin	+	+++
Other markers		
P-53	−	−
Morphology		
Nuclear polymorphism	Moderate	Low
Intratumoral fibrosis	Absent	High
Mitoses	Few	Absent

dpm = disintegrations per minute.

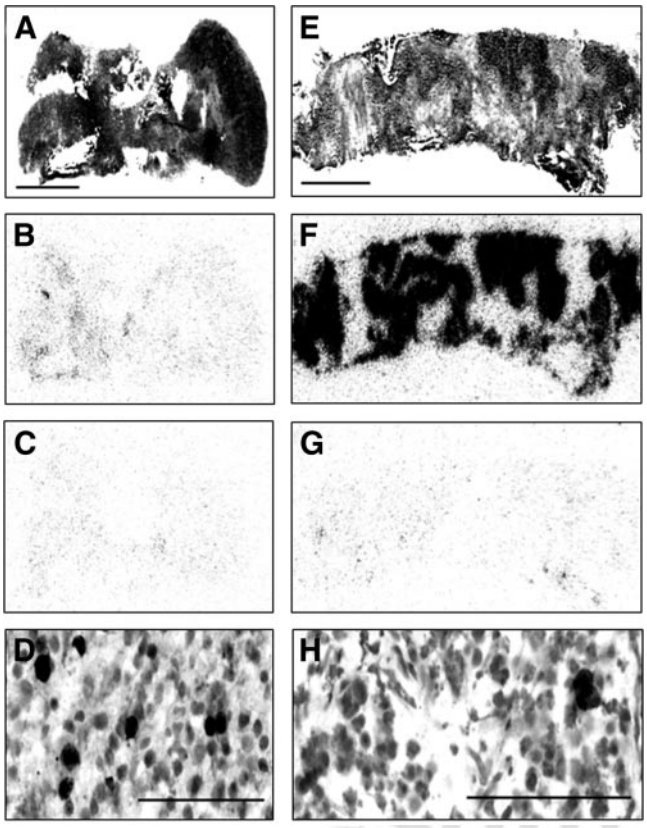

FIGURE 2. Histopathology and receptor autoradiography of somatostatin receptor (SSR)-negative tumor 1 (A, B, C, D) and SSR-positive tumor 2 (E, F, G, H) in patient 1. Hematoxylin and eosin staining (A, E), ^{125}I-Tyr^3-octreotide autoradiography (B, C, G, F) in absence (B, F) and presence (C, G) of excess of unlabeled octreotide, and MIB1 immunohistochemistry (D, H).

only. Figure 2 shows the almost negative results for somatostatin receptors measured with receptor autoradiography.

Tumor 2 was identified as nests of neoplastic cells surrounded by acellular, fibrotic tissue. The nuclei were characterized by less polymorphism and lower proliferative activity (less than 1%) of MIB1-positive cells [Fig. 2] than tumor 1. The cells displayed a strong neuroendocrine differentiation, with highly positive synaptophysin and CD56 as well as chromogranin immunostaining. P-53 staining was negative. No mitotic figures were seen. The amount of nuclear debris was higher in tumor 2 than in tumor 1. The distribution of somatostatin receptors as measured with ^{125}I-Tyr^3-octreotide was homogenous in the tumor tissue and of high density. Fig. 2 shows the somatostatin receptor distribution in the tumor tissue. The high degree of (presumably radiation-induced) fibrosis is well identified in this sample. The fibrotic area is receptor negative. The difference between both tumors in terms of somatostatin receptor density is considerably larger than the differences in morphologic and immunologic characteristics.

An ^{18}F-FDG scan in September 1999 with a coincidence γ-camera identified 4 hot lesions in the liver. As far as correlation between CT and octreotide scan was feasible, ^{18}F-FDG–positive lesions included octreotide-positive as well as octreotide-negative lesions.

After discussion, the patient accepted an additional treatment dose of ^{90}Y-DOTATOC and subsequent chemotherapy. After the fifth dose of ^{90}Y-DOTATOC, he refused a sixth dose. The patient died in mid 2000.

Patient 2

A 66-y-old man was diagnosed with liver metastases of a NET in October 2001. At that time, the primary tumor was not identified. An octreotide scan showed uptake in liver metastases. In December 2001, during surgical radiofrequency ablation (RFA), the presumed primary tumor in the head of the pancreas was identified. The patient underwent 2 more sessions of percutaneous RFA in March and April 2002. A repeat CT scan demonstrated tumor regrowth in formerly ablated lesions. A repeat octreotide scan showed good tracer uptake in the known lesions, which looked "cystic" on CT. From July to December 2002, the patient was treated with a total of 26 GBq ^{177}Lu-DOTA^0,Tyr^3-octreotate (^{177}Lu-DOTATATE) divided over 4 treatment sessions (3 treatments of 7.4 GBq and a final treatment of 3.7 GBq). Uptake in the tumors after the the first therapy was high (Fig. 3). Surprisingly, after the second cycle of 7.4 GBq of ^{177}Lu-DOTATATE, no uptake in the tumors was seen. Because the CT scan at this time appeared unchanged, additional treatments were given, with the same absence of tracer accumulation on scans after therapy. Follow-up CT scans performed 6 wk and 3 mo after the last cycle showed no change in tumor size. On the CT scan performed 6 mo after the last therapy, a slight decrease (about 25%) in measured tumor diameter was found. The octreotide scan at this time showed cold spots, demonstrating that octreotide receptors were absent. A fine-needle biopsy from one of the liver lesions revealed abundant necrotic cell debris, and $<5\%$ of cells appeared to be viable NET.

Patient 3

A 46-y-old man presented with abdominal pain caused by an 8-by-8-by-6-cm NET of the pancreatic tail with macro- and microscopic invasion in the spleen. There was no hormonal syndrome. He subsequently underwent a laparotomy, and the pancreatic tail, spleen, left kidney, and part of the major omentum were removed. Histology showed cytoplasmic immunohistochemical positivity for chromogranin A

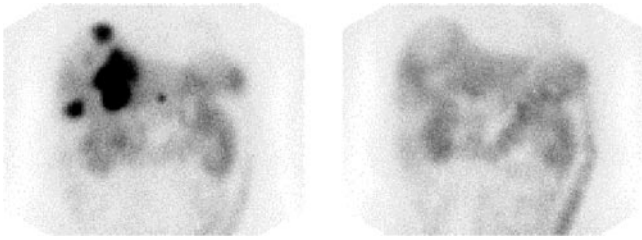

FIGURE 3. Scans acquired 3 d after first (left) and second (right) injection of 7.4 GBq ^{177}Lu-DOTATATE in patient 2, diagnosed with liver metastases of a NET.

and synaptophysin. Immunohistochemistry for neuron-specific enolase (NSE) was variable. MIB-1 expression varied between 5% and 25%. Metastatic lesions were found in the resected part of the omentum. There were no liver metastases. Two years later, he presented with metastases in the stomach, liver, and retroperitoneal lymph nodes. He underwent a subtotal resection of the stomach. The octreotide scan showed high uptake of the radioligand in the residual lymph node and liver metastases. He was subsequently treated with 4 courses of ^{177}Lu-DOTATATE, with a cumulative dose of 30 GBq. This therapy resulted in a complete response, as evidenced by CT and MRI scans (Fig. 4). The octreotide scan showed only a physiologic distribution of the tracer. Routine liver chemistry, chromogranin A, and NSE levels in blood were also within normal limits (Fig. 4). His quality of life was excellent. At the end of 2002, he presented with rapidly progressive liver and lymph node metastases that were not visible on the octreotide scan. Histology confirmed the neuroendocrine nature of the metastases, and immunohistochemistry was negative for sst2. He developed a rapid increase in liver enzymes. Within 1 mo aspartate aminotransferase levels rose from 60 to 285 U/L, alanine aminotransferase levels rose from 60 to 235 U/L, and lactic acid dehydrogenase levels rose from 474 to 1,879 U/L. NSE levels had dramatically increased as well, but serum chromogranin-A levels were only slightly increased (Fig. 4). It was concluded that the patient has a rapidly progressive metastatic neuroendocrine carcinoma with liver metastases and lymph node metastases. There was still no hormonal syndrome. He was referred for chemoembolization. However, at the time of the planned chemoembolization, he had already developed a hepatofugal flow in the portal vein and ascites caused by peritoneal metastases. For this reason, he could undergo only intrahepatic chemotherapy with streptozotocin and paracentesis. This approach resulted in a partial regression of liver metastases and decrease of the elevated liver enzyme levels. He subsequently underwent monthly courses of intravenous chemotherapy with etoposide and cisplatin. This therapy resulted in further partial regression of the liver metastases, improvement of liver enzyme levels, decrease and normalization of the NSE and chromogranin A levels, and disappearance of the ascites. His quality of life improved dramatically. However, he died of metastatic cancer 5 mo after the start of chemotherapy at the age of 50 y.

DISCUSSION

Three patients with NETs are described, with emphasis on tumor size or characteristics according to molecular imaging and tumor histopathology in the setting of applied PRRT and chemotherapy. Table 1 summarizes the findings in the 3 cases.

Patient 1 had multiple metastases that expressed different levels of sst2 receptors, from almost absent to high density. Metastases with high expression of sst2 (thus octreotide scan-positive), responded differently to PRRT than did lesions with very low expression of sst2 and that were octreotide scan-negative. sst2-negative tumors showed clear tumor growth, whereas sst2-positive tumors showed moderate shrinkage on CT (up to 25%–50% at several follow-up time points), which could be explained by clear tumor fibrosis. These opposite results in a single patient are proof of principle that indeed PRRT is peptide receptor–based. Both types of tumors but not all individual lesions were visible on the ^{18}F-FDG scan. The patient died within 18 mo after the last treatment, showing the aggressiveness of such sst2-negative lesions.

Patient 2 had "cystic" GEP NET liver metastases that turned negative on octreotide scan during PRRT, with only moderate change in size according to CT. Histology showed mainly necrotic cell debris with only very few viable neu-

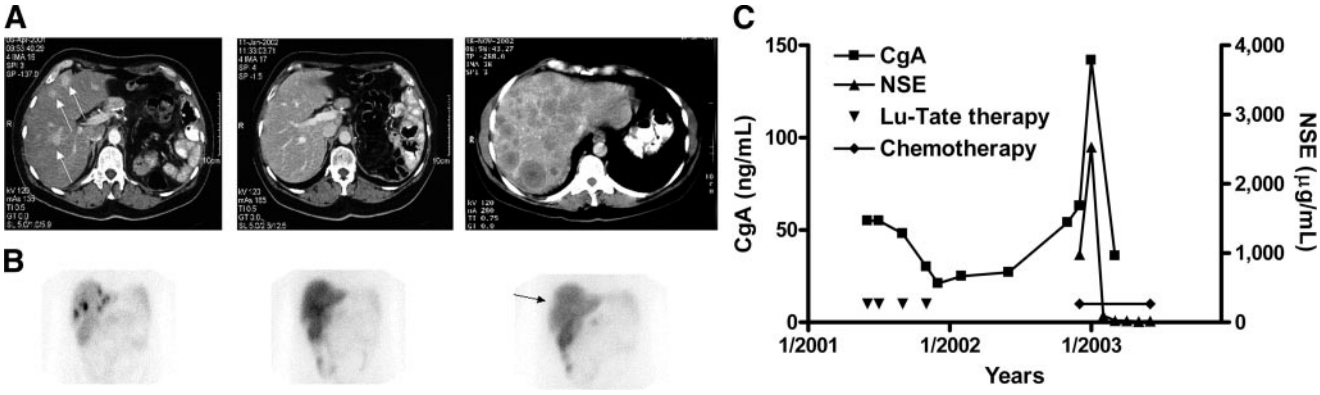

FIGURE 4. (A) CT scans before (left), 3 mo after (middle), and 12 mo after (right) last therapy with ^{177}Lu-octreotate in patient 3 with liver metastases of an operated neuroendocrine pancreatic tumor. Disappearance of tumor sites (arrows, left) at 3-mo follow-up (middle). Recurrence of tumors at 12-mo follow-up (right). (B) Planar scans of abdomen, 3 d after injection of 7.4 GBq ^{177}Lu-octreotate (left and middle) and 1 d after the injection of 222 MBq ^{111}In-octreotide. Image at 3 d shows clear accumulation in tumor sites in liver after first therapy (left) and loss of intensity of uptake in liver lesions after last therapy (middle). Octreotide scan at 3-mo follow-up was negative (right). (C) Course of chromogranin A (CgA; normal upper limit, 100 ng/mL) and neuron-specific enolase (NSE; normal upper limit, 16.3 μg/L) during and after ^{177}Lu-octreotate therapy and chemotherapy.

roendocrine cancer cells, corresponding with successful PRRT treatment.

Patient 3 had a tumor that was initially octreotide scan-positive and responded with complete remission to PRRT with a somatostatin analog. A later recurrence was an octreotide scan-negative, dedifferentiated tumor of a clinically nonfunctioning GEP NET. Rapid progression within weeks and high serum NSE levels were in agreement with the nature of a dedifferentiated tumor (*6*).

These experiences emphasize again that anatomic imaging alone in the follow-up of GEP NETs can indicate that tumors respond to therapy from stabilization in size to partial regression, but that these techniques are not specific to indicate the proportion of or even absence of viable cancer cells inside these tumors. Complete responses to therapy are still rare in GEP NETs. In cases of incomplete responses, tumor volumes on CT or MR imaging may overestimate the actual viable cancer cell volume, at least for the GEP NET. When tumors can still be seen by CT or MR imaging, the presence of cancer cells in such tumors can be demonstrated noninvasively by PRS, PET, or other nuclear imaging using specific cancer cell tracers or invasively by histology. Although the spatial resolution of molecular imaging is increasing, in vivo information about intratumoral heterogeneity of cancer cells cannot be obtained practically at the moment. An idea of intratumoral heterogeneity can be obtained only from rather large tumors (several centimeters in diameter), with spatial resolution on the order of 5 or 15 mm of the best PET and SPECT systems, respectively. It has been reported but not systematically studied, that in about 20% of patients with GEP NETs a second tumor is present in the midgut (*7*). These tumors can be gastrointestinal adenocarcinomas, which are octreotide scan-negative. Therefore, a negative lesion among other positive lesions on an octreotide scan can also represent a (metastasis of a) second tumor, thus again pointing at the importance of performing molecular imaging. In principle, one should thus aim to differentiate such a second tumor from a dedifferentiated GEP NET, because another therapeutic approach may be required. Currently, histology is needed to provide the final answer. It is a challenge for molecular imaging to come up with more smart molecules to do such mapping noninvasively in the future.

Without anatomic information about the presence and size of tumors and if tumors are devoid of the characteristic for which the single radioligand used has been designed (e.g., a certain receptor), PRS and PET will lose their meaning (and thus their clinical relevance). In contrast, because of the high expression and incidence of somatostatin receptors in GEP NET, the octreotide scan has not only a higher sensitivity than CT or MR imaging for this type of tumor (except for benign insulinomas), but it is of clinical relevance even in the absence of CT- or MR-identified lesions (*8–15*). Last, but not least, lesions that are too small (occult disease) will be missed by all imaging techniques.

Table 1 shows when and why molecular imaging was helpful for our understanding of the histopathologic changes after therapy in our 3 patients. The result of an octreotide scan in the absence or presence of (stable or growing) lesions seen on CT or MR imaging may reflect various histopathologic situations. A positive octreotide scan lesion very likely indicates a differentiated GEP NET. A negative lesion may indicate a dedifferentiated GEP NET, as in patient 1. In patient 2 it was the imaging substrate of histologically proven cell necrosis, whereas in patient 3 it reflected a complete remission, later to be followed by the appearance of "cold spots" representing sst2-negative lesions. Such findings with respect to GEP NET differentiation have also been reported on the basis of in vitro data (*3,4*). Accordingly, in patient 3, at the time of CR after PRRT and based on molecular imaging, histology was not necessary for the interpretation of the PRRT response (and also was impossible because the lesions were seemingly absent).

In patient 1, therapy with PRRT with a somatostatin analog showed opposite responses in tumors with or without sst2 receptors. All octreotide positive lesions in the 3 patients responded more or less to PRRT. Patient 3, with a recurrent, octreotide scan-negative, dedifferentiated GEP NET, was treated with chemotherapy with good response.

Little has been reported about the role of molecular imaging in indicating the degree of differentiation of GEP NETs. The initial reports, with one exception, are very promising, pointing to the predictive value of the combination of somatostatin receptor scintigraphy (SRS) and ^{18}F-FDG PET (*16–18*). A flip-flop phenomenon is described, namely SRS-positive/^{18}F-FDG-negative tumors coincide with low human Ki-67 protein, and SRS-negative/^{18}F-FDG-positive tumors coincide with high Ki-67. Ki-67 is a nuclear antigen related to proliferation, and MIB1 is an antibody that binds to this antigen. Thus, the value of Ki-67 is an indication of the aggressiveness of these tumors, with high values pointing to the most aggressive forms with short survival (*19*). With these promising reported results and knowledge about the type of cancer involved, molecular imaging may someday replace invasive pathology during follow-up. With more smart molecules for molecular imaging (that is, more cocktails of peptides for various peptide receptors and ligands directed to fibrosis, apoptosis, necrosis, mRNA, and DNA), the future may lead to a broader application of molecular imaging in in vivo molecular pathology during follow-up.

It is obvious that better-designed, comprehensive studies are needed to show the possible impact of molecular imaging in these tumors as a means of in vivo molecular pathology. Preferably, these studies for this rare tumor type will be performed in global multicenter trials. The recent foundation of the European Neuroendocrine Tumor Society in Budapest, Hungary, with the participation of many disciplines, is a welcome platform for the support of such studies. The global approach, among other things, underlines the

fact that standardization of all techniques (e.g., Society of Nuclear Medicine protocols), histopathology, and other aspects of practice is essential (*9*). Recent introduction of SPECT/CT and PET/CT systems will allow much better reporting of heterogeneity of metastases with respect to different molecular processes, to be studied with various available smart molecules. In addition, the introduction of excellent ^{68}Ge/^{68}Ga generators is promising for affordable PET studies with ^{68}Ga-chelated molecules " from the pipeline" (*20*).

CONCLUSION

When can we rely on molecular imaging during or after therapy cycles for follow-up of a patient with GEP NETs and avoid invasive pathology? Based on the available smart molecules and reported data, this might be a possibility when there is: (a) a decrease in tumor accumulation of radiolabeled octreotide after PRRT cycles, with clear tumor shrinkage shown by CT or MR imaging; and (b) the presence of octreotide scan-negative tumors among positive ones as an indicator of the coexistence of differentiated and dedifferentiated GEP NETs (or, in rare cases, of non-GEP NETs). In the first, the choice of therapy was appropriate, and, in the second, PRRT is not sufficient and chemotherapy is also indicated.

Biopsy and histopathology will remain the mainstays of the initial diagnosis of GEP NET. During follow-up after therapy, molecular imaging is more important in the patient with GEP NET, obviating the need in most instances for classic pathology.

REFERENCES

1. Reubi JC, Waser B, Schaer JC, Laissue JA. Somatostatin receptor sst1–sst5 expression in normal and neoplastic human tissues using receptor autoradiography with subtype-selective ligands. *Eur J Nucl Med.* 2001;28:836–846.
2. Moertel CG, Kvols LK, O'Connell MJ, Rubin J. Treatment of neuroendocrine carcinomas with combined etoposide and cisplatin: evidence of major therapeutic activity in the anaplastic variants of these neoplasms. *Cancer.* 1991;68:227–232.
3. Reubi JC, Kvols LK, Waser B, et al. Detection of somatostatin receptors in surgical and percutaneous needle biopsy samples of carcinoids and islet cell carcinomas. *Cancer Res.* 1990;50:5969–5977.
4. Reubi JC, Chayvialle JA, Franc B, Cohen R, Calmettes C, Modigliani E. Somatostatin receptors and somatostatin content in medullary thyroid carcinomas. *Lab Invest.* 1991;64:567–573.
5. Pauwels S, Barone R, Walrand S, et al. A practical dosimetry of peptide receptor radionuclide therapy with ^{90}Y-labeled somatostatin analogs. *J Nucl Med.* 2005; 46:92S–98S.
6. Baudin E, Gigliotti A, Ducreux M, et al. Neuron-specific enolase and chromogranin A as markers of neuroendocrine tumours. *Br J Cancer.* 1998;78:1102–1107.
7. Modlin IM, Lye KD, Kidd M. A 5-decade analysis of 13,715 carcinoid tumors. *Cancer.* 2003;97:934–959.
8. Lebtahi R, Cadiot G, Sarda L, et al. Clinical impact of somatostatin receptor scintigraphy in the management of patients with neuroendocrine gastroenteropancreatic tumors. *J Nucl Med.* 1997;38:853–858.
9. Balon HR, Goldsmith SJ, Siegel BA, et al. Procedure guideline for somatostatin receptor scintigraphy with ^{111}In-pentetreotide. *J Nucl Med.* 2001;42:1134–1138.
10. De Jong M, Kwekkeboom D, Valkema R, Krenning EP. Radiolabelled peptides for tumour therapy: current status and future directions—plenary lecture at the European Association of Nuclear Medicine 2002. *Eur J Nucl Med Mol Imaging.* 2003;30:463–469.
11. Gibril F, Reynolds JC, Chen CC, et al. Specificity of somatostatin receptor scintigraphy: a prospective study and effects of false-positive localizations on management in patients with gastrinomas. *J Nucl Med.* 1999;40:539–553.
12. Gibril F, Jensen RT. Diagnostic uses of radiolabelled somatostatin receptor analogues in gastroenteropancreatic endocrine tumours. *Dig Liver Dis.* 2004; 36(suppl1):S106–S120.
13. Jamar F, Fiasse R, Leners N, Pauwels S. Somatostatin receptor imaging with indium-111-pentetreotide in gastroenteropancreatic neuroendocrine tumors: safety, efficacy and impact on patient management. *J Nucl Med.* 1995;36:542–549.
14. Krenning EP, Kwekkeboom DJ, Bakker WH, et al. Somatostatin receptor scintigraphy with [^{111}In-DTPA-D-Phe1]- and [^{123}I-Tyr^3]-octreotide: the Rotterdam experience with more than 1000 patients. *Eur J Nucl Med.* 1993;20:716–731.
15. Kwekkeboom DJ, Lamberts SW, Habbema JD, Krenning EP. Cost-effectiveness analysis of somatostatin receptor scintigraphy. *J Nucl Med.* 1996;37:886–892.
16. Adams S, Baum RP, Hertel A, Schumm-Drager PM, Usadel KH, Hor G. Metabolic (PET) and receptor (SPET) imaging of well- and less well-differentiated tumours: comparison with the expression of the Ki-67 antigen. *Nucl Med Commun.* 1998;19:641–647.
17. Adams S, Baum R, Rink T, Schumm-Drager PM, Usadel KH, Hor G. Limited value of fluorine-18 fluorodeoxyglucose positron emission tomography for the imaging of neuroendocrine tumours. *Eur J Nucl Med.* 1998;25:79–83.
18. Belhocine T, Foidart J, Rigo P, et al. Fluorodeoxyglucose positron emission tomography and somatostatin receptor scintigraphy for diagnosing and staging carcinoid tumours: correlations with the pathological indexes p53 and Ki-67. *Nucl Med Commun.* 2002;23:727–734.
19. Rindi G, Bordi C. Highlights of the biology of endocrine tumours of the gut and pancreas. *Endocr Relat Cancer.* 2003;10:427–436.
20. Maecke HR, Hofmann M, Haberkorn U. ^{68}Ga-labeled peptides in tumor imaging. *J Nucl Med.* 2005;46:172S–178S.